

## Controlled photoluminescence in amorphous-silicon-nitride microcavities

Ali Serpengüzel, and Selim Tanriseven

Citation: *Appl. Phys. Lett.* **78**, 1388 (2001); doi: 10.1063/1.1347022

View online: <https://doi.org/10.1063/1.1347022>

View Table of Contents: <http://aip.scitation.org/toc/apl/78/10>

Published by the [American Institute of Physics](#)

---

### Articles you may be interested in

[Photoluminescence of Si-rich silicon nitride: Defect-related states and silicon nanoclusters](#)

*Applied Physics Letters* **90**, 131903 (2007); 10.1063/1.2717014

[Photoluminescence from silicon nitride—no quantum effect](#)

*Journal of Applied Physics* **110**, 023520 (2011); 10.1063/1.3607975

[Emission properties of high- \$Q\$  silicon nitride photonic crystal heterostructure cavities](#)

*Applied Physics Letters* **93**, 021112 (2008); 10.1063/1.2958346

[Gap states in silicon nitride](#)

*Applied Physics Letters* **44**, 415 (1984); 10.1063/1.94794

[Investigation of charge trapping centers in silicon nitride films with a laser-microwave photoconductive method](#)

*Applied Physics Letters* **62**, 615 (1993); 10.1063/1.108873

[Microstructure and properties of silicon nitride thin films deposited by reactive bias magnetron sputtering](#)

*Journal of Applied Physics* **83**, 5831 (1998); 10.1063/1.367440

---



The image shows a Measure Ready M91 FastHall Controller, a compact, silver-colored electronic device. It features a color LCD screen displaying four test results: Continuity (Not run), Contact Check (2019-01-01 at 01:59, 2637 ms), Resistivity (2019-01-01 at 01:59, 1058 ms), and FastHall™ (17.44). The device has a 'Measure Ready' indicator and 'M91 FastHall' branding on the front panel.

**Measure Ready**  
**M91 FastHall™ Controller**

A revolutionary new instrument  
for complete Hall analysis

 Lake Shore  
CRYOTRONICS

## Controlled photoluminescence in amorphous-silicon-nitride microcavities

Ali Serpengüzel<sup>a)</sup>

Physics Department, Koç University, Sariyer, Istanbul 80910, Turkey

Selim Tanriseven

Physics Department, Bilkent University, Bilkent, Ankara 06533, Turkey

(Received 23 August 2000; accepted for publication 12 December 2000)

Narrow-band and enhanced photoluminescence have been observed in hydrogenated amorphous-silicon-nitride microcavities. The distributed Bragg reflectors were fabricated using alternating layers of hydrogenated amorphous-silicon nitride and hydrogenated amorphous-silicon oxide. The microcavity resonance wavelength was designed to be at the maximum of the bulk hydrogenated amorphous-silicon-nitride luminescence spectrum. At the microcavity resonance, the photoluminescence amplitude is enhanced, while the photoluminescence linewidth is reduced with respect to the bulk hydrogenated amorphous-silicon nitride. © 2001 American Institute of Physics. [DOI: 10.1063/1.1347022]

The ability to control the emission properties of semiconductors with optical microcavities and photonic band-gap materials is continuing to attract the attention of the photonics community.<sup>1</sup> As they alter the properties of the optical gain media, optical microcavities can be used in very low-threshold lasers and very efficient light-emitting diodes (LEDs).<sup>2</sup>

Optical microcavities have also been applied to porous silicon ( $\pi$ -Si), after the observation of room-temperature visible photoluminescence (PL) made  $\pi$ -Si a potential optical gain medium.<sup>3</sup> Microcavity-controlled PL in  $\pi$ -Si has been observed experimentally<sup>4</sup> and calculated theoretically.<sup>5</sup> Microcavity-controlled electroluminescence (EL) of  $\pi$ -Si has also been reported.<sup>6</sup> Optical waveguides have been formed from  $\pi$ -Si,<sup>7</sup> and two-dimensional photonic crystals have been fabricated in  $\pi$ -Si optical waveguides.<sup>8</sup>

Similar to  $\pi$ -Si, hydrogenated amorphous silicon ( $a$ -Si:H) also exhibits room-temperature visible PL.<sup>9</sup> In addition, planar waveguides are being realized from  $a$ -Si:H.<sup>10</sup> An advantage of  $a$ -Si:H is that it can be deposited by plasma-enhanced chemical-vapor deposition (PECVD) on almost any substrate at temperatures below 500 K, which makes it potentially compatible with microelectronic technology. These developments justify the renewed interest in silicon (Si) as a potential optoelectronic material. With modern process techniques, it will be possible to integrate lasers, photodetectors, and waveguides into optoelectronic Si motherboards.<sup>11</sup>

Recently, we have observed room-temperature visible PL from  $a$ -Si:H nitride ( $a$ -SiN<sub>x</sub>:H).<sup>12</sup> The efficiency of the PL from  $a$ -SiN<sub>x</sub>:H is approximately 3%, which agrees well with previously published results for  $a$ -Si:H.<sup>13</sup> We have also observed the enhancement of PL in a planar  $a$ -SiN<sub>x</sub>:H microcavity realized with metallic mirrors.<sup>14</sup> While the exact mechanism of the occurrence of the PL in bulk  $a$ -SiN<sub>x</sub>:H is still under discussion, we have suggested<sup>12</sup> the use of a quantum-confinement model.<sup>15</sup> There, it was proposed that

our samples consist of small  $a$ -Si clusters in a matrix of  $a$ -SiN<sub>x</sub>:H. The regions with Si-H and Si-N, having larger energy gaps due to strong Si-H and Si-N bonds, isolate these  $a$ -Si clusters, and form barrier regions around them. The PL originates from the  $a$ -Si clusters.

In this letter, we report the control of PL in an all-dielectric  $a$ -SiN<sub>x</sub>:H microcavity. The microcavity is realized by sandwiching the active  $a$ -SiN<sub>x</sub>:H layer between two distributed Bragg reflectors (DBRs). The microcavity resonance wavelength was designed to be at the maximum (710 nm) of the bulk  $a$ -SiN<sub>x</sub>:H luminescence spectrum.

The microcavity was realized by a  $\lambda/2$  active (i.e., luminescing) layer of  $a$ -SiN<sub>x</sub>:H sandwiched between two passive DBR mirrors. As found in our previous studies, the presence of the ammonia (NH<sub>3</sub>) in growth determines whether the  $a$ -SiN<sub>x</sub>:H will be active or passive. First, the passive bottom DBR was deposited by PECVD on the Si substrate using 14 pairs of  $\lambda/4$  alternating layers of  $a$ -SiN<sub>x</sub>:H (with refractive index=1.72 and metric thickness=104 ± 5 nm) and  $a$ -SiO<sub>x</sub>:H (with refractive index=1.45 and metric thickness=124 ± 6 nm). For the passive  $a$ -SiN<sub>x</sub>:H deposition, ammonia (NH<sub>3</sub>) with a flow rate of 10 sccm, and 2% silane (SiH<sub>4</sub>) in nitrogen (N<sub>2</sub>) with a flow rate of 180 sccm were used. For the passive  $a$ -SiO<sub>x</sub>:H deposition, nitrous oxide (N<sub>2</sub>O) with a flow rate of 25 sccm, and 2% SiH<sub>4</sub> in N<sub>2</sub> with a flow rate of 180 sccm were used. After the deposition of the bottom DBR, a  $\lambda/2$  layer of active  $a$ -SiN<sub>x</sub>:H (with refractive index=2.03 and metric thickness = 163 ± 8 nm) was deposited. For the active  $a$ -SiN<sub>x</sub>:H deposition, only 2% SiH<sub>4</sub> in N<sub>2</sub> with a flow rate of 180 sccm was used. Afterwards, the top DBR was deposited, using 14 pairs of  $\lambda/4$  alternating layers of  $a$ -SiO<sub>x</sub>:H and  $a$ -SiN<sub>x</sub>:H. The radio-frequency power was 20 W, and the deposition chamber pressure 1 Torr during the continuous deposition process. Figure 1 shows a schematic of the  $a$ -SiN<sub>x</sub>:H microcavity. The  $\lambda/4$  passive  $a$ -SiN<sub>x</sub>:H layers are shown in black, while the  $\lambda/4$  passive  $a$ -SiO<sub>x</sub>:H layers are shown in white. The  $\lambda/2$  central layer of active  $a$ -SiN<sub>x</sub>:H is shown in gray.

Figure 2 shows the measured room-temperature reflectance (upper curve) and PL (lower curve) spectra of the

<sup>a)</sup>Author to whom correspondence should be addressed; electronic mail: aserpenguzel@ku.edu.tr

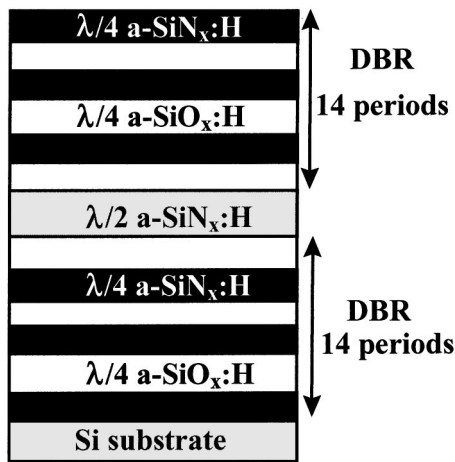


FIG. 1. Schematic of the  $a\text{-SiN}_x\text{:H}$  microcavity with DBR mirrors.

$a\text{-SiN}_x\text{:H}$  microcavity. The room-temperature reflectance and PL measurements were made at  $0^\circ \pm 5^\circ$  with respect to the surface normal with a resolution of 0.1 nm. The PL spectra were later corrected for the responsivity of the spectrometer and the photomultiplier tube. An  $\text{Ar}^+$  laser with a wavelength of 514.5 nm and a power of 150 mW was focused with a 15 cm focal length cylindrical lens on the samples. During the PL measurements the temperature of the sample is not controlled and there might be local heating, which reduces the PL efficiency and broadens the PL linewidth.<sup>16</sup> However, local heating would not considerably affect the general shape and features of the  $a\text{-SiN}_x\text{:H}$  gain spectrum. As seen in the PL spectra of Fig. 3, even though there might be local heating, we are observing strong PL from the sample.

There is good agreement between the reflectance and the PL spectra. Both the reflectance and the PL spectra of Fig. 2 show a microcavity resonance at a wavelength of 710 nm. This resonance has a linewidth of  $\Delta\lambda = 6$  nm and a quality factor of  $Q = 118$ . The PL is enhanced by the microcavity resonance, which correlates well with the minimum of the reflectance spectrum.

In order to clarify the effect of the microcavity and to demonstrate its advantages with respect to the bulk  $a\text{-SiN}_x\text{:H}$ , we also show the PL of a  $\lambda/2$ -thick layer of bulk  $a\text{-SiN}_x\text{:H}$  (dotted line) in Fig. 3, obtained under the same experimental conditions. The red–near-infrared PL of the

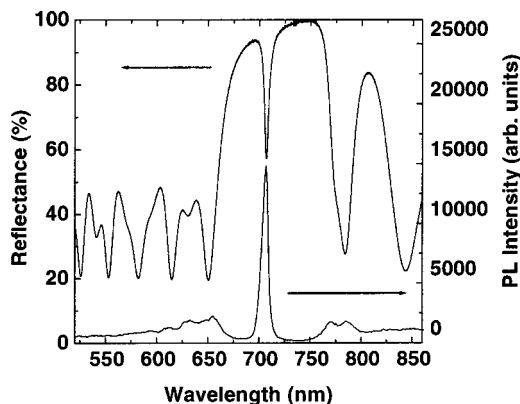


FIG. 2. Experimental reflectance (upper curve) and PL (lower curve) spectrum of the  $a\text{-SiN}_x\text{:H}$  microcavity.

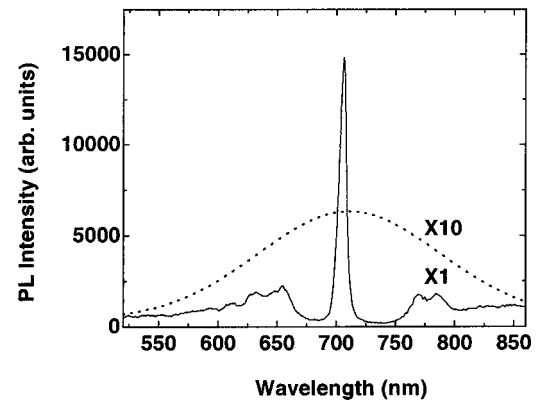


FIG. 3.  $1\times$  PL spectrum of the  $\lambda/2$   $a\text{-SiN}_x\text{:H}$  microcavity (solid line) and  $10\times$  PL spectrum of the  $\lambda/2$  bulk  $a\text{-SiN}_x\text{:H}$  (dotted line).

bulk  $a\text{-SiN}_x\text{:H}$  has a broad linewidth of 240 nm. This broad linewidth shows that  $a\text{-SiN}_x\text{:H}$  has potential as a photonic gain medium.

A comparison of the spectra in Fig. 3 shows that the effect of the microcavity is twofold: first, the wide emission band (240 nm) is strongly narrowed to 6 nm; second, the resonant enhancement of the peak PL intensity is more than one order of magnitude with respect to the emission of the  $\lambda/2$ -thick layer of bulk  $a\text{-SiN}_x\text{:H}$ . In addition, by choosing the appropriate width of the  $a\text{-SiN}_x\text{:H}$  active layer and DBRs, it is possible to select the emission wavelength of the microcavity by taking advantage of the broad spectral emission of the  $a\text{-SiN}_x\text{:H}$  active layer.

In conclusion, we have demonstrated that  $a\text{-SiN}_x\text{:H}$  microcavities with DBR mirrors can be successfully realized by PECVD, and can be used for the control of the PL in  $a\text{-SiN}_x\text{:H}$ . The PL of the  $a\text{-SiN}_x\text{:H}$  is both narrowed and enhanced at the microcavity resonance with respect to the PL of the bulk  $a\text{-SiN}_x\text{:H}$ . This narrowing and enhancement of the PL can be understood by the redistribution of the density of optical modes due to the presence of the microcavity. The microcavity narrowing and enhancement of luminescence in  $a\text{-SiN}_x\text{:H}$  opens up a variety of possibilities for optoelectronic applications such as resonant cavity enhanced LEDs.

The authors would like to acknowledge the partial support of this research by the North Atlantic Treaty Organization (NATO), Grant No. SfP-971970 and the Scientific and Technical Research Council of Turkey (TUBITAK), Grant No. TBAG-1952.

- <sup>1</sup> *Microcavities and Photonic Band Gaps: Physics and Applications*, edited by J. Rarity and C. Weisbuch (Kluwer, Dordrecht, 1996).
- <sup>2</sup> R. E. Slusher and C. Weisbuch, *Solid State Commun.* **92**, 149 (1994).
- <sup>3</sup> T. Canham, *Appl. Phys. Lett.* **57**, 1046 (1990).
- <sup>4</sup> L. Pavesi, C. Mazolleni, A. Tredicucci, and V. Pellegrini, *Appl. Phys. Lett.* **67**, 3280 (1995).
- <sup>5</sup> E. K. Squire, P. St. J. Russell, and P. A. Snow, *Appl. Opt.* **37**, 7107 (1998).
- <sup>6</sup> M. Araki, H. Koyama, and N. Koshida, *Appl. Phys. Lett.* **69**, 2956 (1996).
- <sup>7</sup> H. F. Arrand, T. M. Benson, P. Sewell, and A. Loni, *J. Lumin.* **80**, 199 (1999).
- <sup>8</sup> S. W. Leonard, H. M. van Driel, K. Busch, S. John, A. Birner, A.-P. Li, F. Müller, U. Gösele, and V. Lehmann, *Appl. Phys. Lett.* **75**, 3063 (1999).
- <sup>9</sup> D. J. Wolford, B. A. Scoot, J. A. Reimer, and J. A. Bradley, *Physica B* **117**, 920 (1983).
- <sup>10</sup> A. M. Agarwal, L. Liao, J. S. Foresi, M. R. Black, X. Duan, and L. C. Kimerling, *J. Appl. Phys.* **80**, 6120 (1996).

- <sup>11</sup>A. Kaneko, T. Goh, H. Yamada, T. Tanaka, and I. Ogawa, *IEEE J. Sel. Top. Quantum Electron.* **5**, 1227 (1999).
- <sup>12</sup>A. Aydinli, A. Serpengüzel, and D. Vardar, *Solid State Commun.* **98**, 273 (1996).
- <sup>13</sup>D. J. Wolford, B. A. Scott, J. A. Reimer, and J. A. Bradley, *Physica B* **117B&118B**, 920 (1983).
- <sup>14</sup>A. Serpengüzel, A. Aydinli, A. Bek, and M. Güre, *J. Opt. Soc. Am. B* **15**, 2706 (1998).
- <sup>15</sup>M. H. Brodsky, *Solid State Commun.* **36**, 55 (1980).
- <sup>16</sup>R. Fisher, in *Amorphous Semiconductors*, edited by M. H. Brodsky (Springer, Berlin, 1985), pp. 159–187.